Eur. Phys. J. D **13**, 317–322 (2001)

THE EUROPEAN PHYSICAL JOURNAL D

EDP Sciences

Intensity and detuning dependence of fine structure changing collisions in a ^{85}Rb magneto-optical trap

M.W. Mancini, A.L. de Oliveira[a], K.M.F. Magalhães, V.S. Bagnato, and L.G. Marcassa[b]

Instituto de Física de São Carlos, Universidade de São Paulo, Departamento de Física e Ciência dos Materiais, Caixa Postal 369, 13560-970 São Carlos, SP Brazil

Received 4 May 2000 and Received in final form 11 October 2000

Abstract. This paper reports on an experimental investigation of fine structure changing collisions between cold and trapped ^{85}Rb atoms. Our previous work [Eur. Phys. J. D **7**, 317 (1999)] reported on our assessment of the contribution of FSC to the total trap loss using photoionization by a cw laser to detect the atomic fragments in the $5P_{1/2}$ state originating from these collisions. The Doppler effect plays an important role in the detection scheme and had a limiting effect on our previous experiment. To overcome this problem, we have used a pulsed laser in this work. The signal/noise ratio was improved, allowing us to measure the intensity and frequency dependence of the loss rate due to FSC. A comparison of our results with the semiclassic Gallagher-Pritchard model revealed some disagreements, for which we propose several arguments to attempt to explain these discrepancies. We believe that these results should stimulate theoretical work on this field.

PACS. 32.80.Pj Optical cooling of atoms; trapping – 33.80.Ps Optical cooling of molecules; trapping – 34.50.Rk Laser-modified scattering and reactions

1 Introduction

Collisions between cold and trapped atoms have been extensively studied over the last decade for all alkali atoms [1–3]. Inelastic cold collisions in the presence of radiation fields may result in hot atoms, which may have sufficient kinetic energy to escape from a magneto-optical trap (MOT), thus leading to atomic losses. Two main loss mechanisms are believed to be dominant at a higher laser intensity: Radiative Escape (RE) and Fine Structure Changing (FSC) collisions. Both mechanisms involve the encounter of a ground and an excited state atom. The radiative escape (RE) process begins when two ground state atoms, interacting through a van der Walls interaction, (C_6/R^6), in the presence of the laser radiation field, absorb a photon of frequency ω when far apart from each other. The colliding pair thus formed is promoted to a long range dipole-dipole attractive potential, $(-C_3/R^3)$, asymptotically correlated to the atomic states $5S_{1/2} + 5P_{3/2(1/2)}$. In this potential, the atoms are accelerated against each other. Spontaneous decay may occur during this motion because the collisional time is longer than the excited state lifetime. The pair emits a photon (ω') shifted to the red of the atomic transition (ω), and the energy difference $\hbar(\omega - \omega')$ is transferred to kinetic energy which, in a homonuclear collision, is shared equally between the two atoms. The main effect of the decay process is radiative heating (RH). If the energy gained is insufficient for the pair to escape, the dissipative mechanisms of the trap will be sufficient to cool the heating undergone by the atoms. On the other hand, if the energy gained is greater than the trap's depth, ∼1 K, the atoms will escape from the trap. Fine structure changing (FSC) is a second channel, which starts like the RE, *i.e.*, the pair of atoms begin the collision while they are both in the ground state, absorbing a trapping laser photon, and go to an excited molecular state asymptotically connected to the atomic states $5S_{1/2}+5P_{3/2}$. If spontaneous decay does not occur during the acceleration, the quasimolecule will survive in the excited molecular state, reaching short internuclear separations. In this region, non-adiabatic transitions to another potential correlated, at long range, to the $5S_{1/2} + 5P_{1/2}$ state may occur through the pseudocrossing between the two molecular potential curves. For most of the alkali, except Li, the energy difference between the fine levels ($nP_{3/2}$ and $nP_{1/2}$) of the nP state transferred into kinetic form is sufficient to cause the loss of both the colliding atoms. For Rb, this energy corresponds to $\Delta_{\rm FSC}/k_{\rm B} = 342$ K.

Early investigations explored the total trap loss rate by measuring the total collisional loss rates as a function

[a] *Permanent address:* Departamento de Física, Universidade Federal de São Carlos and Universidade do Estado de Catarina, Brazil.

[b] e-mail: `marcassa@if.sc.usp.br`

of light intensity [4,5] and frequency using the catalysis technique [6]. One of the main points of interest in inelastic cold collisions is the fact that they can limit the total number of trapped atoms and the atomic density in a MOT; both parameters play an important role in the achievement and understanding of the Bose-Einstein Condensation [7–9] and in the realization of the photoassociative spectroscopy of molecular states, which requires high densities [10–12]. Discriminating between the two dominant loss mechanisms is important because can lead to a better understanding of the inelastic cold collisions, that still remain, mainly theoretically, not fully understood. According to Dashevskaya *et al.* [13] and Julienne and Vigué [14], in the case of heavy dimers such as the Rb_2 quasimolecule, the FSC loss mechanism is believed to occur mainly at short internuclear separations in which the exchange interaction dominates all the others (resonant dipole-dipole, Coriolis and spin-orbit). In this case, the main contribution for these loss mechanisms originates in the transition at $R \approx 10a_0$, through the radial coupling between the two attractive states $0_u^+(A^1\Sigma_u^+)$ and $0_u^+(b^3\Pi_u)$ of the Rb_2 molecule, both correlated to the dissociation limit 5S + 5P induced by the spin-orbit interaction. Another crossing occurs at long range, between the curves of the $0_u^+(5S_{1/2} + 5P_{3/2})$ state, and the attractive 1_u correlated asymptotically to the atomic states $5S_{1/2}+5P_{1/2}$, in $R \approx 23a_0$, through the Coriolis interaction. However, the latter possibility is believed [14] not to contribute significantly to FSC losses because the probability of FSC occurring through this long range crossing, which is inversely proportional to the pair's reduced mass, is very small for heavy dimers. It is important, however, for lighter species such as Li and Na. One can calculate the FSC probability using the Landau-Zener formula [15] for non-adiabatic transition probabilities, $P_{\mathrm{LZ}} = 2\mathrm{e}^{-A}(1 - \mathrm{e}^{-A})$, where the adiabaticity parameter $A = 2\pi\Omega^2/hvD$ gives a measure of the coupling between the molecular states $A^1\Sigma_u^+$ and $b^3\Pi_u$ through the spin-orbit interaction; v is the relative velocity of the atoms in the quasimolecule and D is the difference between the slopes of the potential curves, both evaluated at the crossing point. We used $\Omega = 81\ \mathrm{cm}^{-1}$ [14], while the other parameters required to evaluate the FSC probability were obtained from the adiabatic potential curves for Rb_2 [16]. The value of parameter A was determined at 0.248, leading us to obtain $P_{\mathrm{LZ}} = 0.34$, which is in good agreement with the reference [14] ($P_{\mathrm{LZ}} = 0.36$).

Until quite recently, only a few research groups had come up with techniques to individually measure RE and FSC [17–19]. However, much still remains to be done. Three earlier studies were carried out to directly observe the FSC process. In the work of Fioretti *et al.* [19], the losses in a Cs MOT induced by these collisions were measured directly by excitation of the atoms through a D2 line and the detection of the fluorescence yield on the D1 line. In their experiment with K atoms, Wang and collaborators [20] used-ionization to detect the product of an FSC collision, measuring the trap loss spectra and also estimating the line broadening caused by the predissociation of the 1_g and 0_u^+ states. From these investigations they concluded that the main contribution to the loss process comes from the 0_u^+ state. It should be pointed out that ion detection is more efficient than photon counting, since the detection efficiency of the former is close to 100% while the efficiency of the latter is restricted, among others, by the factor containing the solid angle available to the photomultiplier. Shaffer and co-workers recently worked out a fluorescence measurement-based experiment to determine the FSC contribution to trap-loss in a Cs MOT [19], providing a comparison with the experiment of Fioretti *et al.* [18]. In a previous experiment [17] our group measured the contribution of FSC to the total trap-loss rate by ionizing the atomic fragments in the $5P_{1/2}$ state. In this sense, our procedure was similar to the experimental detection scheme used by Wang [20], the main difference being that [17] we also obtained the value for the contribution of the FSC process to the total loss. Ionization was performed by cw lasers (a combination of a dye laser and a krypton ion laser) and a rate equations model had to be used to obtain the fraction of the $5P_{1/2}$ state population. This was necessary because the excitation from the $5P_{1/2}$ state to the $8S_{1/2}$ state could, by spontaneous decay, populate other levels (7P, 6P and 5P, and by cascade to 7S, 6S, 5S, 5D and 4D). The Doppler effect also played an important role in this experiment. The Doppler width of $5P_{1/2} \rightarrow 8S_{1/2}$ transition is approximately 600 MHz, due to the different velocities at which the $P_{1/2}$ fragments come out, and the narrow cw laser ($\Delta\nu \sim 1$ MHz) was only able to interact with a very narrow velocity class from the distribution, producing only a few atoms. The result was a very small signal, due to the reduced production of ions and an integrating technique was necessary to collect all the velocity class contribution.

In this work, the FSC collisional loss rate was measured through the ionization of the $5P_{1/2}$ atomic fragments generated in these collisions using a nanosecond pulsed dye laser. The pulsed laser presents a large linewidth ($\Delta\nu \sim 6$ GHz) and sufficiently high intensity to enable it to interact with all the atoms from the outgoing velocity distribution. The high intensity of this laser also overcomes the decay from the $8S_{1/2}$ state to other levels, precluding the need to use rate equations to evaluate the actual population in the $5P_{1/2}$ level. The significant improvements introduced by the pulsed laser technique have enabled us to perform experiments to measure the intensity and frequency dependence of the FSC mechanism. Our results were compared with previous work and the possible effects of hyperfine structures were observed.

2 Experimental setup and detection scheme

The experimental set up is schematized in Figure 1. Our MOT operates in a closed stainless steel vapor cell [21]. The Rb vapor from a reservoir maintained at $-20\ ^\circ\mathrm{C}$ effuses through a valve into the main chamber kept at a background pressure of 10^{-10} torr. Three mutually orthogonal, retroreflected laser beams from an injection-locked diode laser tuned to 5 MHz of the red of the atomic $5S_{1/2}(F = 3) \rightarrow 5P_{3/2}(F' = 4)$ transition intersect at

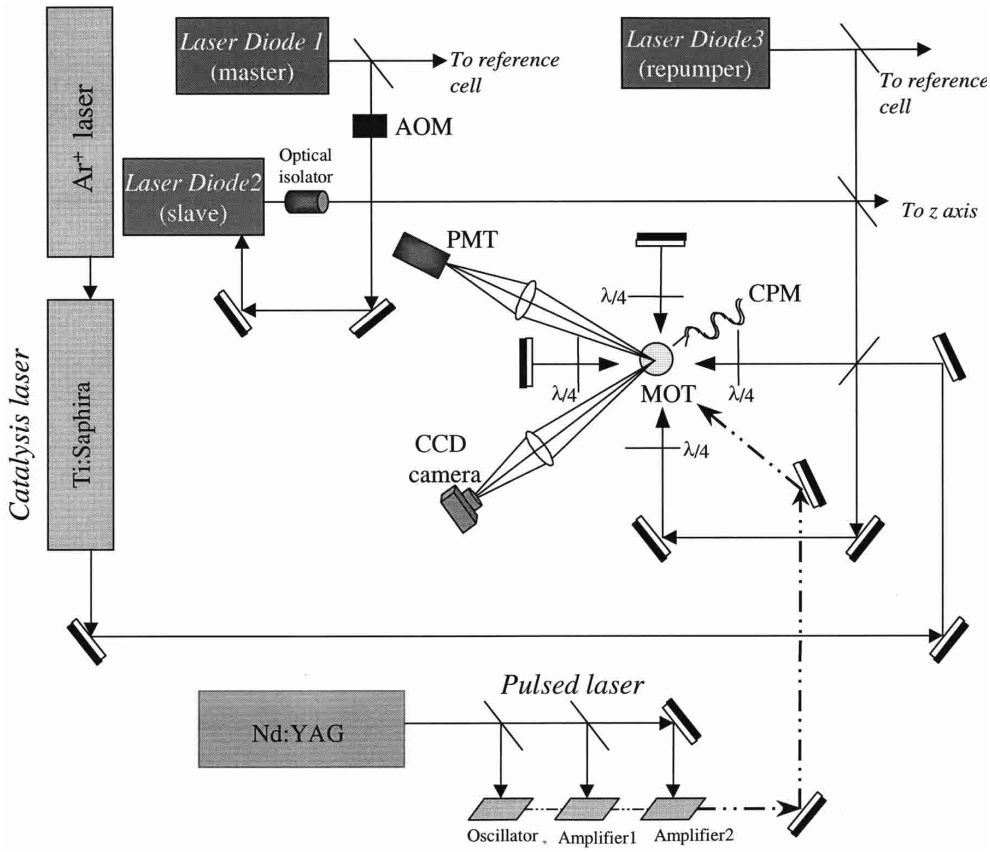

Fig. 1. Schematic diagram of the experimental setup used in both intensity and catalysis experiments, showing the lasers used to ionize the atomic fragments generated in the FSC collisions, and the additional catalysis laser. Also are shown the diode lasers used in the trapping of Rb atoms.

the center of the quadruple magnetic field generated by a pair of anti-Helmholtz coils. The magnetic field coils are located outside the chamber and produce an axial field gradient of about 10 Gauss/cm near the center. A diode laser, tuned to the $5S_{1/2}(F = 2) \rightarrow 5P_{3/2}(F' = 3)$ transition, works as a repumper preventing the population from leaving the main trap-transition. The maximum total trap intensity was about 50 mW/cm^2. This configuration of static magnetic field and light field, with appropriate laser polarization, creates an environment that traps and cools atoms to about 200 μK. The number of trapped atoms is measured by imaging their fluorescence onto a calibrated photomultiplier (PMT) and the volume of the cloud can be derived from images taken with a charge couple device (CCD) camera. These two values are used to calculate the atomic density. Under our conditions, the total number of atoms was $N \sim 10^7$ atoms and the density was in the order of 10^{10} cm^{-3}. A precise measurement of atomic density is taken for each intensity or detuning.

After the colliding pair in the $5S_{1/2} + 5P_{3/2}$ potential has been transferred to the $5S_{1/2} + 5P_{1/2}$, it is excited to the $5S_{1/2} + 8S_{1/2}$ state and subsequently promoted to the continuum by a second similar photon of the pulsed dye laser (1 mJ/pulse, 4 ns, repetition rate 10 Hz, $\lambda \sim 607$ nm) pumped by the second harmonic of an Nd:YAG laser (Continuum-Surelite I). The atoms leaving the trap, due to FSC, exit at a velocity that can be as high as 130 m/s in every spatial direction. Because of this spatial spread, the $5P_{12} \rightarrow 8S_{12}$ transition has a Doppler width of approximately 600 MHz. Hence, if a cw dye laser is used (typically 1 MHz linewidth) to excite this transition, the number of atoms emerging in the $P_{1/2}$ that is accessed will be very small owing to the Doppler profile. On the other hand, the use of a pulsed laser with a large spectral bandwidth ensures that the laser reaches all the atoms within the velocity distribution. For the second transition, which ionizes atoms out of $8S_{1/2}$, connecting them to the continuum, the Doppler broadening poses no problem because of the large power broadening that exists in this transition. The ions are detected by a channeltron particle multiplier (CPM) and discriminated by an ion counter. Indeed, only the atoms in the $P_{1/2}$ state, which compose the quasimolecules, are ionized and can be easily detected and counted.

Three different tests were carried out to ensure that the detected ions actually originated from atoms in the $5P_{1/2}$ state. The first test consisted of a time of flight (TOF) measurement. Using the $5P_{1/2} \rightarrow 8S_{1/2}$ transition, we measured the TOF for Rb^+ and Rb_2^+ ions. This calibration procedure allowed us to ensure that the ions detected in the experiment were atomic rather than molecular. The second test consisted of verifying the pulsed laser intensity dependence of the ion signal. A quadratic dependence was observed, suggesting that ionization is a two photon process consistent with the transitions involved. The last test consisted of obtaining the spectrum of the ion signal around the wavelength $\lambda \approx 607$ nm and confirmed that the ions start at the $5P_{1/2} \rightarrow 8S_{1/2}$ transition.

3 Intensity dependence

In contrast to the previous experiment [17], in which our use of a cw dye laser allowed us to measure the rate at which atoms were leaving the MOT in the $5P_{1/2}$, the analysis using a pulsed laser is entirely different because most of the time the probe laser is turned off. Therefore, we did not measure the production rate of $5P_{1/2}$ atoms. We were only able to obtain an average population for this level during the periods when the probing laser pulses were turned on. The population is governed by the following rate equation:

$$\frac{dN_{p_{1/2}}}{dt} = \frac{1}{2}\beta_{FSC} n_c N - \Gamma N_{p_{1/2}} \quad (1)$$

where β_{FSC} is the contribution of FSC to the total loss, n_c is the atomic density in the sample, N is the total number of trapped atoms, $N_{p_{1/2}}$ is the atomic population in the $5P_{1/2}$ level and Γ is the spontaneous decay rate out of the $5P_{1/2}$. In the steady state situation we have:

$$N_{p_{1/2}} = \frac{1}{2\Gamma}\beta_{FSC} n_c N. \quad (2)$$

Through a calibration procedure similar to the one employed in reference [17], we determined that each laser pulse ionizes almost 100% of the atoms in the $5P_{1/2}$ level. For an intensity of 35 mW/cm^2, we counted 37.0 ± 0.5 ions for 200 laser pulses. This gave us an average population, in the $5P_{1/2}$ level, of $\langle N_{p_{1/2}} \rangle = 0.185 \pm 0.003$ atoms. For these conditions, together with the measured trap parameters, we obtain $\beta_{FSC} = (1.78 \pm 0.53) \times 10^{-12}$ cm^3/s. The entire procedure can be repeated for several trap laser intensities employed; the intensity dependence of β_{FSC} is shown in Figure 2, where the error bars are originated from the errors in the volume and total atoms number measurements. From a qualitative standpoint, this behavior was already expected since the excited state population increases with intensity and, therefore, the loss rate β, which involves a ground state and an excited state atom, increases. To compare our results with calculations, we employed the Gallagher-Pritchard (GP) model [22], which has proved to be reliable in several situations. It is, however, a simple model which serves only to make comparisons of the overall behavior, while comparisons of the absolute values for the loss rate require more sophisticated models. One can observe, from Figure 2, that the experimental points decrease much faster as the intensity decreases than predicted by the GP model (plotted in this figure as a full solid line), which was scaled in order to be compared with the experimental results. We believe that this discrepancy may be due to the fact that the FSC process depends on the hyperfine level occupied by the ground state atom involved in the collision. Because the intensity of the trapping laser was varied while the repumper intensity was kept constant ($I_r = 30$ mW/cm^2) in this study, there were variations in both the excited state population and the relative distribution of the population in the two hyperfine ground states. As the intensity of the trapping laser decreases, the fraction of population in the hyperfine ground

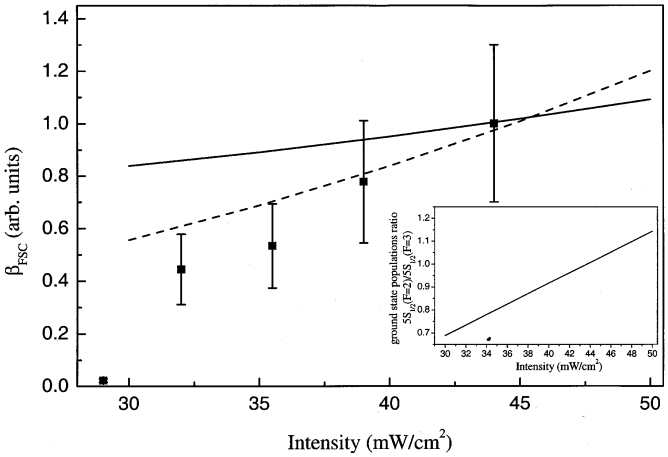

Fig. 2. Intensity dependence of the FSC loss rate. The GP theoretical curve is shown as a full line; the improved model based on the hyperfine ground populations in the $5S_{1/2}(F = 2)$ and $5S_{1/2}(F = 3)$ states is represented by the dashed line. For both models, the results were scaled in order to be compared with the experimental data. The inset shows the ratio between the two hyperfine ground state populations in the $5S_{1/2}(F = 2)$ and $5S_{1/2}(F = 3)$.

state of higher energy ($F = 3$) also increases because the strong repumper pumps the atoms from the lower ground state $F = 2$ to $F = 3$. It is known, from theory [16], that the $5S_{1/2}(F = 2) + 5P_{3/2}$ state is more favorable for FSC than the $5S_{1/2}(F = 3) + 5P_{3/2}$ state because the 0_u^+ potential, which is the most favorable for FSC, is connected asymptotically to the $5S_{1/2}(F = 2) + 5P_{3/2}$ state. This fact had already been observed in our previous work [17]. Therefore, the loss rate coefficient β, which depends on the excited state population and on the hyperfine ground state population in $F = 2$, is expected to decrease faster than given in the prediction. In order to improve the GP model we have considered that it depends on the product of the excited state population and also the population on the $5S_{1/2}(F = 2)$ state. To obtain the population distribution in the hyperfine ground states, we have used a rate equation model that includes four levels ($5S_{1/2}(F = 2)$, $5S_{1/2}(F = 3)$, $5P_{3/2}(F = 3)$ and $5P_{3/2}(F = 4)$) and two laser frequencies, the trapping laser close to the $5S_{1/2}(F = 3) \rightarrow 5P_{3/2}(F' = 4)$ transition and repumper laser close to the $5S_{1/2}(F = 2) \rightarrow 5P_{3/2}(F' = 3)$ transition. In the inset of Figure 2, we show the ratio between the populations in the two hyperfine ground states ($5S_{1/2}(F = 2)$ and $5S_{1/2}(F = 3)$). Including the effect of the ground state population, we found there was a much better agreement between this model (full line) and the experimental points. The dashed line of Figure 2 represents the improved model.

In terms of absolute value, the present experiment indicates that $\beta_{FSC} \approx 0.35\beta$, *i.e.*, the contribution of the FSC mechanism to the total loss in the trap is about 35%. Comparing these with our earlier results for Rb [17], we find that this value is higher than the previous one. In this present experiment, the pulsed dye laser used

to excite the $P_{1/2}$ fragments has a broad spectral range ($\Delta\nu \sim 6$ GHz). Therefore, not only $P_{1/2}$ atoms can be ionized but also molecular states connected asymptotically to the $5S_{1/2}+5P_{1/2}$ state. This corresponds to exciting atomic pairs at internuclear separations from $200a_0$ to $2500a_0$. In this broad range of excitation, not only separated atoms near the dissociation limit but also molecules, which would never produce atoms in the $5P_{1/2}$ state, due to spontaneous decay, become excited and ionized. This would, in fact, increase the ion count, resulting in a larger contribution of FSC to total loss when compared with the cw excitation. Based on these arguments, we shall state that $\beta_{\rm FSC} \approx 0.35\beta$ is believed to be closer to reality than our previous work.

4 Frequency dependence: catalysis results

The traditional catalysis experiments [6] use an additional laser to introduce losses in the cold atomic sample. The frequency and intensity of this laser are simultaneously varied in order to obtain the frequency dependence of β, which is achieved by keeping the additional loss constant. Had we followed this procedure for our pulsed probe experiment, we would have had to keep the number of ions/pulse constant. However, this would have meant that, for each frequency, we would have had to accumulate data for a long period until we had adjusted the intensity to keep the number of ions/pulse constant. Because it introduces excessively intense fluctuations, this procedure produces gross errors in the measurement. This procedure is similar to the one described in reference [6]. To avoid these errors, we kept the catalysis laser intensity ($I_{\rm c} = 4.4$ mW/cm^2) constant and scanned its frequency within the interval of -1200 MHz $\leq \Delta \leq -50$ MHz from the $5S_{1/2}(F=3) \rightarrow 5P_{3/2}(F'=4)$ transition, measuring the additional ion production. The number of ions/pulses shows a linear dependence on the intensity of the catalysis laser. Now, in the presence of the catalysis laser, the population in the $5P_{1/2}$ level ($N'_{\rm p_{1/2}}$) is related to the losses through equation [23]:

$$N'_{\rm p_{1/2}} = \frac{1}{2\Gamma}(\beta_{\rm FSC} + \beta^{\rm c}_{\rm FSC}) n'_{\rm c} N' \qquad (3)$$

where $n'_{\rm c}$, N', and $N'_{\rm p_{1/2}}$ are, respectively, the atomic density, total number of trapped atoms and the population in the $5P_{1/2}$ state in the presence of the catalysis laser. $\beta^{\rm c}_{\rm FSC}$ is the loss rate due to FSC introduced by the catalysis laser. Using the result of equation (2), the additional losses introduced by the catalysis laser to FSC ($\beta^{\rm c}_{\rm FSC}$) is given by:

$$\beta^{\rm c}_{\rm FSC} = 2\Gamma \left(\frac{N'_{\rm p_{1/2}}}{n'_{\rm c} N'} - \frac{N_{\rm p_{1/2}}}{n_{\rm c} N} \right) \qquad (4)$$

where $n_{\rm c}$, N, and $N_{\rm p_{1/2}}$ are, respectively, the atomic density, the total number of trapped atoms and the population in the $5P_{1/2}$ in the absence of catalysis. Extracting

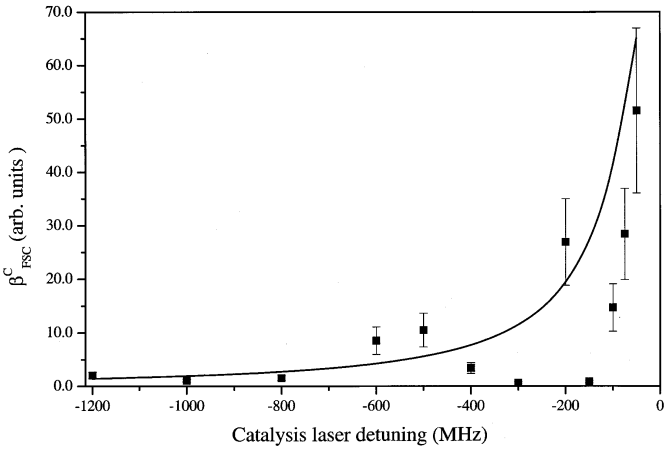

Fig. 3. Additional trap loss rate due to FSC introduced by the catalysis laser, $\beta^{\rm c}_{\rm FSC}$, as a function of catalysis laser detuning, operating below the transition $5S_{1/2}(F=3) \rightarrow 5P_{3/2}(F'=4)$; in the frequency range of -1200 MHz $\leq \Delta_{\rm c} \leq -50$ MHz. The full line represents the theoretical prediction.

$\beta^{\rm c}_{\rm FSC}$ from the experimental results, we obtained the results shown in Figure 3. For $\Delta = -50$ MHz of the catalysis laser, we observed that $\beta^{\rm c}_{\rm FSC}$ is about the same order of $\beta_{\rm FSC}$. It should be pointed out that large fluctuations were observed between -300 MHz and -150 MHz similar to those originally observed by Walker and co-workers [6]. Applying the GP model with frequency variation, we observed a strong disagreement, mainly in small detunings, between the model (full line) and the experimental result, which is ascribed to the simplicity of the model. The main assumption, in the model, is that losses occur through a single channel represented by one attractive potential curve in the form of $-C_3/R^3$, where C_3 is a mean value. In our calculations we used $C_3 = 18.4$ a.u., from the results of Marinescu [24]. In fact, there are many curves with different C_3 coefficients in the small detuning region, which are caused by hyperfine interaction [25, 26]. The spectrum of Figure 3 presents two minima, one at -300 MHz and the other at -150 MHz. This region is very complex, presenting several potential crossings including hyperfine repulsive states. We believe that, in this region, the catalysis laser is exciting the atomic colliding pair either to a repulsive hyperfine potential or to a pure long-range state [27,28]. In both these possibilities, the number of pairs that undergo FSC decrease, possibly causing the deep dips in the spectrum of $\beta^{\rm c}_{\rm FSC}$. In the large detuning region the model and experimental results agree well. An overall important observation is that the frequency dependence of the FSC process shows a completely different behavior when compared with the total loss, which has already been reported in the literature. We observed peculiar oscillations in $\beta^{\rm c}_{\rm FSC}$ which are not present in the total trap loss rate. This may suggest that the hyperfine interaction plays an important role in this loss process. Nevertheless, the understanding of its influence is a complex task to be carried out experimentally and theoretically.

5 Conclusions

In this work we took direct measurements of the contribution to the loss rate of trapped atoms in an ^{85}Rb MOT induced by the FSC collisional process. The technique involves ionization, by a pulsed laser, of the atomic fragments generated in these collisions. The trapping laser intensity and frequency dependence of the FSC process were studied. In the case of intensity dependence, we found evidence that the FSC process depends on both the excited state and the hyperfine ground state population. In the catalysis type experiment, we observed the manifestation of the hyperfine interaction on the excited states. We concluded that repulsive and pure long-range states may play an important role in the frequency dependence of the FSC process. Our current laboratory investigations of fluctuation may lead to a better understanding of this phenomenon. We trust our findings will stimulate the development of theories capable of dealing with the complexity of the molecular hyperfine structure.

This work was supported by the Brazilian research funding institutions FAPESP, Programa PRONEX and CNPq. Our special thanks are extended to R. Napolitano for helpful comments. We also would like to thanks J. Weiner for technical support.

References

1. J. Weiner, V.S. Bagnato, S.C. Zilio, P.S. Julienne, Rev. Mod. Phys. **71**, 1 (1999).
2. J. Weiner, Adv. At. Mol. Opt. Phys. **35**, 45 (1995).
3. K.-A. Suominen, J. Phys. B: At. Mol. Opt. Phys. **29**, 5981 (1996).
4. M. Prentiss, A. Cable, J. Bjorkholm, S. Chu, E. Raab, D. Pritchard, Opt. Lett. **13**, 452 (1988).
5. L. Marcassa, V. Bagnato, Y. Wang, C. Tsao, J. Weiner, O. Dulieu, Y. Band, P.S. Julienne, Phys. Rev. A **47**, R4563 (1993).
6. D. Hoffmann, P. Feng, R.S. Willianson III, T. Walker, Phys. Rev. Lett. **69**, 753 (1992); D. Hoffmann, P. Feng, T. Walker, J. Opt. Soc. Am. B **11**, 7112 (1994).
7. M.H. Anderson, J.R. Ensher, M.R. Matthews, C.E. Wieman, E.A. Cornell, Science **269**, 198 (1995).
8. C.C. Bradley, C.A. Sackett, R.G. Hulet, Phys. Rev. Lett. **78**, 985 (1997).
9. K.B. Davis, M.-O. Mewes, M.R. Andrews, N.J. van Druten, D.S. Kurn, W. Ketterle, Phys. Rev. Lett. **75**, 582 (1995).
10. R.A. Cline, J.D. Miller, D.J. Heinzen, Phys. Rev. Lett. **73**, 632 (1994); *ibid.* **71**, 2200 (1993).
11. P.D. Lett, K. Helmerson, W.D. Phillips, L.P. Ratliff, S.L. Rolston, M.E. Wagshul, Phys. Rev. Lett. **71**, 2200 (1993); L.P. Ratliff, M.E. Wagshul, P.D. Lett, S.L. Rolston, W.D. Phillips, J. Chem. Phys. **101**, 2638 (1994).
12. H. Wang, P.L. Gould, W.C. Stwalley, Phys. Rev. A **53**, R1216 (1996).
13. E.I. Dashevskaya, A.I. Veronin, E.E. Niktin, Can. J. Phys. **47**, 1237 (1969).
14. P.S. Julienne, J. Vigué, Phys. Rev. A **44**, 4464 (1991).
15. C. Zener, Proc. R. Soc. Lond. A **137**, 696 (1932).
16. O. Dulieu, P.S. Julienne, J. Weiner, Phys. Rev. A **49**, 607 (1994); O. Dulieu, private communication.
17. L.G. Marcassa, R.A.S. Zanon, S. Dutta, J. Weiner, O. Dulieu, V.S. Bagnato, Eur. Phys. J. D **7**, 317 (1999).
18. J.P. Shaffer, W. Shalupczak, N. Bigelow, Eur. Phys. J. D **7**, 323 (1999).
19. A. Fioretti, J.H. Müller, P. Verkerk, M. Allegrini, E. Arimondo, P.S. Julienne, Phys. Rev. A **55**, R3999 (1997).
20. H. Wang, P. Gould, W. Stwalley, Phys. Rev. Lett. **80**, 476 (1998).
21. C. Monroe, W. Swann, H. Robinson, C. Wieman, Phys. Rev. Lett. **65**, 1571 (1990).
22. A. Gallagher, D. Pritchard, Phys. Rev. Lett. **63**, 957 (1989).
23. D. Sesko, T. Walker, C. Monroe, A. Gallagher, C. Wieman, Phys. Rev. Lett. **63**, 961 (1989).
24. M. Marinescu, A. Dalgarno, Phys. Rev. A **52**, 311 (1995).
25. C.J. Willians, P.S. Julienne, J. Chem. Phys. **101**, 2634 (1994); C.J. Willians, E. Tiesinga, P.S. Julienne, Phys. Rev. A **53**, R1939 (1996).
26. T. Walker, D. Pritchard, Laser Phys. **4**, 1085 (1994).
27. W.C. Stwalley, Y.-H. Uang, Phys. Rev. Lett. **41**, 1164 (1978).
28. V.S. Bagnato, J. Weiner, P.S. Julienne, C.J. Willians, Laser Phys. **4**, 1062 (1994).